RSC Advances

ROYAL SOCIETY OF CHEMISTRY

www.rsc.org/advances

RSC Advances

ARTICLE

The isotopic effects of ^{13}C-labeled fullerenes of large carbon cages (C_{70}) and their formation process

Received 00th April 2015,
Accepted 00th April 2015

DOI: 10.1039/x0xx00000x

www.rsc.org/

Chenglong Wang,[‡ac] Longfei Ruan,[‡a] Xue-Ling Chang,[*a] Xiaoliang Zhang,[b] Sheng-Tao Yang,[*ab] Xihong Guo,[a] Hui Yuan,[a] Cuibin Guo,[a] Weiqun Shi,[a] Baoyun Sun[a] and Yuliang Zhao[a]

Fullerene, C_{60} and its derivatives have been fully investigated and commercialized. The importance of the large carbon cage-based fullerenes for the biomedical applications were gradually recognized due to their fantastic biological effects. In nanotoxicology, the key detection technique was able to retain the intrinsic structure and properties of nanomatrials in biological background. However, it was a puzzled question how to get facilely the detectable fullerene nanomaterials and their formation process. In this study, ^{13}C-enriched fullerenes of large carbon cage, C_{70}, were synthesized in a large scale from ^{13}C-enriched raw carbon material by arc-discharge method. The stable isotopes ^{13}C were directly incorporated into the skeleton of the fullerenes cages without destroying their intrinsic structures. The isotopic effects of ^{13}C-labeled C_{70} were investigated in detail. The ^{13}C labeled amounts of C_{70} was about 7 % higher than that of natural abundance, which greatly improved the ^{13}C detection signal in isotope ratio mass spectrometry and apparent 8-fold carbon nuclear magnetic resonance signal enhancement of fullerenes. The ^{13}C-enriched fullerenes showed significant isotopic effects, such as the strongest peak position shift up (m/z＞840) and the Poisson distribution of isotopic peaks in the mass spectra, the migration or splitting of infrared and Raman characteristic peaks. Comparison of the ^{13}C labeled amounts and isotopic effects of ^{13}C-enriched C_{70} and those of ^{13}C-enriched C_{60}, the formation dynamics of fullerenes were different with the changes of carbon cage, lower carbon cage fullerenes were easily generated in the process of arc-discharge, the ^{13}C stable isotopic effects in high carbon fullerenes were also slight weak. Moreover, these important isotopic effects of ^{13}C-enriched fullerene will facilitate the development of new analytical methods for carbon nanomaterials in vivo.

Introduction

Fullerenes, one category of the most popular carbon nanomaterials, have been widely used in solar energy, cosmetics, personal care, electronics and biomedicine due to their unique chemical and physical properties.[1-7] Their biological efficiency depends on both the modification on the cage and the cage size (C_{60}, C_{70}, C_{82}, etc.). To date, pristine C_{60} and their functionalized derivatives have been fully investigated and commercialized. The large carbon cage-based fullerenes possess more fantastic biological significance. For instance, C_{70} and their derivatives exhibited higher photodynamic therapy and antioxidation efficiency due to the much more extended conjugated π-system of the cage, which can efficiently absorb electrons.[8-12] Metallofullerenes of larger carbon cages (e.g. Gd@C_{82} and Gd@$C_{82}(OH)_x$) also showed promises as radiotracers, magnetic resonance imaging (MRI) contrast reagents and anticancer drug with high-efficacy and low-toxicity.[13-18] Obviously, these biomedical investigations of fullerene nanomaterials, especially for the large carbon cage-based fullerenes, are very significant.[19] Inevitably, the related health and safety issues of fullerene nanomaterials have become urgent.[20-23] Nevertheless, the principal issue is how to realize to quantitatively trace or detect intrinsic carbon nanomaterials in vivo.

Compared with C_{60}, the synthesis and chemical structure of the large carbon cage-based fullerenes were less investigated, especially for the detectable labeled fullerene nanomaterials, including the large-scale synthesis of the labeled fullerenes and influences of labeled groups, etc. Actually, it is very difficult to directly and quantitatively detect fullerene nanomaterials in vivo, because of the high carbon background in environmental and biological systems, the lack of specific detection signal of carbon nanomaterials and the complexity of biological matrixes.[24] Currently, radioactive labeling and fluorescent modification have been adopted to quantify fullerenes nanomaterials in vivo.[25-32] Although these labeling methods have high sensitivity and specificity, radioactive labeling suffers some inescapable drawbacks, such as the strict conditions of radioactivity operation and the generation of radioactive wastes. Separately, fluorescent groups easily

[a.] CAS Key Laboratory for Biomedical Effects of Nanomaterials and Nanosafety, Institute of High Energy Physics, Chinese Academy of Sciences, Beijing 100049, P. R. China. changxl@ihep.ac.cn
[b.] College of Chemistry and Environment Protection Engineering, Southwest University for Nationalities, Chengdu, 610041, P. R. China. yangst@pku.edu.cn
[c.] Northwest University, Xi'an, 710075, P. R. China.
† Electronic Supplementary Information (ESI) available. See
DOI: 10.1039/x0xx00000x
‡ C. L. Wang and L. F. Ruan contributed equally.

detach away from the modified nanomaterials or are quenched during the exposure to environmental and biological systems. In addition, metallofullerenes, as higher temperature superconductors, redox active systems, and contrast agents etc., have been investigated.[14, 15, 33-40] However, the properties and structures of fullerenes can be significantly altered by metal inside the carbon cage.[33-40] The synthetic amount of metallofullerenes is also far less than fullerenes. Therefore, stable isotopic labeling is a good choice, which overcomes many drawbacks aforementioned.[41-50]

Stable isotopic labeling combined with the high sensitivity and accuracy of isotope ratio mass spectrometry (IRMS) can provide information about the geographic, chemical and biological origins of substances, and has been widely used in diverse disciplines such as archaeology, medicine, geology, biology, food authenticity and forensic science for several decades.[43-47, 51-53] The ^{13}C stable isotope can be incorporated into the skeletons of these carbon nanomaterials. ^{13}C stable isotopes are used to investigate the structural properties and the formation mechanism of fullerenes nanomaterials.[54-65] We have demonstrated previously the ^{13}C stable isotopic labeling of carbon nanotubes (CNTs), carbon quantum dots and C_{60} for in vivo quantitative biodistribution studies.[48-50] The ^{13}C stable isotopes labeled directly on the skeleton of these carbon nanomaterials do not damage their stability and intrinsic structures. Therefore, the invaluable ^{13}C stable isotopic tracers can reflect the real properties of carbon nanomaterial in biological systems and can also be potentially used as internal standard substance. The feasible ^{13}C stable isotopic labeled technology will promote the development of carbon nanomaterials in nanotoxicology.

In the present work, C_{70}, as an example of large carbon cage-based fullerenes, the ^{13}C-labeled C_{70} were synthesized in a large-scale from ^{13}C-enriched raw carbon material by the arc-discharge method. The stable isotope ^{13}C directly substituted for the carbon atoms of the fullerene cages. The ^{13}C-labeled C_{70} samples were separated and purified through preparative high performance liquid chromatography (HPLC). The numbers of ^{13}C-atoms per C_{70} cage were determined by IRMS. The isotopic effects of ^{13}C-labeled fullerenes were studied in detail by mass spectrometry (MS), carbon nuclear magnetic resonance (CNMR), Fourier transform infrared (IR), Raman spectroscopy and electrochemical system. The obtained ^{13}C-enriched fullerenes, as tracer or a potential internal standard substance, will be very important for the biosafety and biomedical development of fullerenes nanomaterials in future.

Experimental

Preparation of ^{13}C-enriched fullerenes

^{13}C-enriched fullerenes were prepared by arc-discharge method.[54, 59, 66-69] Briefly, the anode electrodes were fabricated by coring out natural-abundance carbon rods and packing them with isotopic enriching amorphous carbon powder (Cambridge Isotopes, 99% ^{13}C). The cathode was a pure graphite rod. The arc discharge was performed under He atmosphere (135 Torr) with the following parameters: interelectrode distance: 5 mm; current: 110 A; voltage 27 V. Fullerene without labeling was prepared following the same protocol by using normal carbon (98.5 % ^{12}C) as starting material.

Separation and purification of ^{13}C-enriched fullerenes

The carbon soot-containing fullerenes were collected and refluxed in CS_2 for 10 h to extract the ^{13}C-enriched fullerene. The ^{13}C-enriched fullerene was further separated and purified by high performance liquid chromatography (HPLC, LC908-C_{60} , Japan Analytical Industry Co.) with toluene as the mobile phase at a flow-rate of 15.0 mL/min and employing a Buckyprep column (20 mm×250 mm, Nacalai Co., Japan), equipped with a UV detector (wavelength, 335 nm).

Determination of ^{13}C-amounts in ^{13}C-enriched fullerenes

IRMS can precisely measure the relative abundance of stable isotopes. Samples are converted into gas and then ionized. Subsequently, the ionized gases with different m/z values are separated under magnetic field and quantified by the detectors. By comparing the detected isotopic ratios to an isotopic standard, an accurate determination of the isotope composition of the sample is obtained. So, it can eliminate any bias or systematic error in the measurements. For example, carbon isotope ratios are measured relative to the internationally recognized C standard Vienna Pee Dee Belemnite (VPDB) and are reported in the delta notation, δ,

$$\delta = \frac{{}^{13}C/{}^{12}C_{sample} - {}^{13}C/{}^{12}C_{standard}}{{}^{13}C/{}^{12}C_{standard}} \times 1000$$

where the $^{13}C/^{12}C_{standard}$ ratio of the VPDB standard sample was 0.0112372. Aliquots of 0.2000±0.0100 mg fullerene samples were weighed into Φ 3.2×4 mm tin cups for stable isotope analysis. Urea as a working standard in practical operation, analyses of carbon isotopes were carried out using a Finnigan MAT-253 (Thermo Electron-Finnigan, USA) continuous-flow isotope ratio mass spectrometer (ConFlo III, Finnigan MAT) coupled with a Flash Elemental Analyzer 1112 (Finnigan, Flash EA 1112 series).

Investigation of isotopic effects in ^{13}C-enriched fullerenes

The detection of ^{13}C incorporation is achieved by measuring the isotopic distribution and shift caused by the slightly heavier ^{13}C-atoms. The isotopic effects of obtained fullerene samples were dissolved in toluene and characterized by the matrix-assisted laser desorption ionization time-of-flight mass spectrometry (MALDI-TOF-MS, Autoflex, Bruker Co., Germany) under negative ion mode, and microprobe Raman spectroscopy (Renishaw inVia plus, Renishaw, UK) under the conditions of excitation wavelength 514 nm, 0.5% laser power, 4 cycles and exposure 50 seconds. The powders of fullerene samples were ground into the KBr pellets under appropriate pressure for Fourier transform infrared spectroscopy (IR, Tensor 27, Bruker, Germany). The fullerenes samples for CNMR were dissolved in an excess of toluene-d_8 and evaporated at 25℃ until saturation was achieved. Using a 30-deg pulse and a 20-s pulse delay, a total of 30720 accumulations obtained over 48 h on a Bruker AV 400 instrument (400 MHz, Switzerland) gave a spectrum with an acceptable signal/noise ratio, showing clearly the presence of

fullerene. The analysis and comparison of all data were normalized by mathematics method of Origin software (OriginPro 8.0). For electrochemical measurements, 4.5 mg C_{70} were dissolved in 10 mL acetonitrile /toluene (volume ratio: 1: 4) under 30 minutes of ultrasound, and containing 0.1 M tetrabutylammonium perchlorate ($TBAClO_4$) electrolyte. A CHI604E electrochemical workstation (Shanghai, China) was used for cyclic voltammetric (CV). A three-electrode cell was used with an Ag/AgCl as the reference electrode, a Pt wire as the counter electrode, and a glassy carbon as the working electrode. The cyclic voltammetry were recorded by a linear potential scan at a sweep rate of 50 mV/s. High-purity nitrogen was purged for 10 min before the test was performed, the potential range was form -2.0 to 0 V. All electrochemical experiments were performed at 25±1 °C.

Results and discussion

Separation and purification of ^{13}C-enriched fullerenes

Buckyprep preparative column can be well satisfied with the separation and enrichment of fullerene nanomaterials. CS_2 solvent extracts-containing fullerenes were separated into C_{60}, C_{70}, C_{76}, C_{82} and C_{96} on the column in 100 minutes. There was a clear resolution of the C_{60} and C_{70} (R_s> 2) without the interferences from endogenous sources (Fig. 1). The retention times of C_{60} and C_{70} were 11.707 and 18.355 min, respectively. Herein, we did not observe the effect of stable isotope ^{13}C labeling on the skeleton of carbon cages to the chromatographic retention time in fullerenes. ^{13}C-enriched fullerenes and normal fullerenes are of the same chromatographic behaviour. The yield of pure ^{13}C-enriched C_{70} was about 2~3 % relative to the discharged soot.

MS analysis

The HPLC isolated fullerenes were identified by MALDI-TOF-MS. The mass spectra for the purified ^{13}C-enriched fullerenes and fullerenes are showed Fig. 2. Normal C_{70}, due to the high abundance of ^{12}C in nature, had the dominating peak at 840 (*m/z*), and was consisted with the theoretical calculation. The C_{70} with a high purity of greater than 99.5% were achieved. The ^{13}C isotopes were labeled on the skeleton of fullerenes. MS spectra of the ^{13}C-enriched C_{70} indicated clearly a statistical distribution of isotopes abundance. As shown in Fig. 2, compared to the C_{70}, the highest peak of ^{13}C-enriched C_{70} shifted in the case ^{13}C from 840.18 (m/z) to 845.75 (m/z). The isotopic distributions in the MS spectra were widened from 840 to 855 (m/z) and displayed extremely well the Poisson distribution. These experimental evidences were similar to those reported in the literature.[55, 58, 59] The MS of ^{13}C-enriched C_{60} were compliant with our previous reports.[69] In addition, we also found other high carbon fullerenes (such as ^{13}C-enriched C_{76}, C_{82} and C_{96}) appeared similar results. The stable ^{13}C isotope enriched the isotopes distribution of mass spectrum and the composition of carbon elements of fullerenes. The isotopic effect of ^{13}C-enriched fullerenes clearly changed the isotopes distribution in MS.

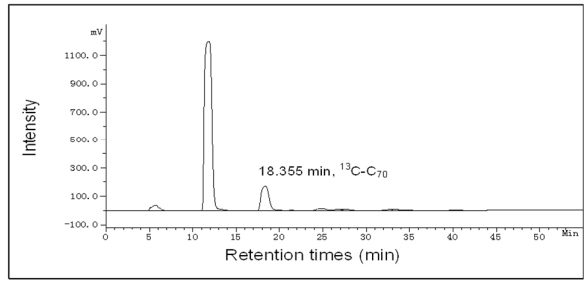

Fig. 1. Separation and purification of ^{13}C-enriched fullerenes.

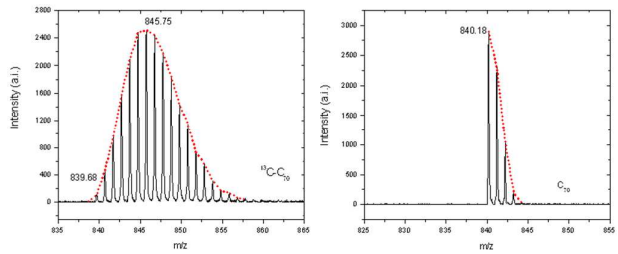

Fig. 2. MS spectra of ^{13}C-C_{70} (left) and C_{70} (right).

Table 1. ^{13}C/^{12}C isotope ratios of ^{13}C-enriched C_{70}.

The addition of ^{13}C in raw carbon powder (%)	$\delta^{13}_{C/}{}^{12}_{C}$	^{13}C/^{12}C (%)	^{13}C-enriched C_{70}
0	-17.436	1.087	C_{70}
15	7211.047	8.408	$^{13}C_5C_{65}$

IRMS analysis

Generally, the stable isotope labeling is combined with IRMS, which is a specialization of mass spectrometry and can precisely measure the relative abundance of stable isotopes, then quantify ^{13}C in fullerenes. ^{13}C is an environmental and non-radioactive isotope of carbon in nature. It makes up about 1.1% of all natural carbon on earth. IRMS can detect the ratio of ^{13}C to ^{12}C of the test samples, which is very sensitive for the addition of ^{13}C isotope in fullerene. IRMS measured the δ of ^{13}C-enriched C_{70} from the different carbon isotope proportion of synthetic materials (the mass ratio of ^{13}C-powder/^{12}C-rod was 15:85). The δ signal showed an increment of about 7000 with ^{13}C/^{12}C increasing only 5 percentages in abundance ratio (Table 1).

The numbers of ^{13}C labeling on the skeleton of fullerene were calculated and estimated by equation:

$$n = \frac{^{13}C\,/\,^{12}C}{1 + {}^{13}C\,/\,^{12}C} \times n_{carbon}$$

The value n_{carbon} is the total carbon number of fullerenes cages. ^{13}C-enriched C_{70} are expressed as $^{13}C_nC_{(70-n)}$. The numbers of ^{13}C atoms in a ^{13}C-enriched C_{70} molecule was 5, meaning as $^{13}C_5C_{65}$. Compared to normal C_{70}, the abundance of ^{13}C in ^{13}C-labeled fullerenes was about ~7 % higher than that of natural abundance. Stable isotope ^{13}C may be randomly distributed in the carbon cage.[56] The ^{13}C labeled amounts of ^{13}C-enriched

C_{70} was less ~2 % than that of ^{13}C-enriched C_{60} in our previous reports.[69] The mixed carbon powders needed to be packed close and uniform. Generally, the extractions from the discharged carbon soot include many high carbon fullerenes (such as C_{76}, C_{82} and C_{96} etc.) except C_{60}. During the process of discharge, the packed ^{13}C powder was utilized dispersedly by the variety of fullerene carbon cages and other carbon substances (e.g. graphite, graphene, carbon nanoparticles). ^{13}C was also labeled in other more high carbon fullerenes of the discharged carbon soot. So, the numbers of ^{13}C in C_{60} or C_{70} were less than the proportion of the starting materials. Comparison of the ^{13}C labeled amounts in ^{13}C-enriched C_{70} and C_{60}, we found obviously that ^{13}C was easily utilized by low carbon fullerene. We sought to understand the formation process of fullerenes that low carbon fullerene was more easily generated and the construction of fullerenes probably originated from small carbon cage in the process of arc-discharge. The speculations were consistent with the report.[55, 56, 59, 61, 64] The skeleton ^{13}C-labeling technique facilitated to explore the formation mechanism of fullerenes and other carbon materials.[54-65] However, the skeleton ^{13}C-labeled fullerenes were obtained largely from direct addition of stable isotope in the origin by arc-discharge method. The ^{13}C labeling was stable without introducing other outside atoms onto the carbon-networks. In the future, we believe that it is significant for exploring and optimizing the synthesis process to improve the ^{13}C labeled amount in fullerenes.

NMR analysis

NMR spectroscopy is a powerful research technique for investigating the physical and chemical properties of chemical molecules (range from small compounds to large proteins or nucleic acids). The CNMR spectra for ^{13}C-enriched C_{70}, shown in Fig. 3, was consisted of five lines with intensities in the ratio 10:20:10:20:10, with chemical shifts of 130.5, 145.0, 147.0, 147.7, and 150.3 ppm, as reported by Johnson et a1..[61, 70] The spectra strongly confirmed the D_{5h} C_{70} structure with five chemically distinct kinds of carbon atoms, in good agreement with the spectrum of C_{70}. In addition, all carbon atoms in the C_{60} molecule were chemical equivalent, the CNMR spectrum for C_{60} was a single line at 143 ppm (in both liquids and solids).[71-74] The single-resonance CNMR spectrum of C_{60} was also a strong evidence for the icosahedral symmetry of this molecule. In a magnetic field, the addition of ^{13}C resulted in that NMR active nuclei enhanced the absorption of electromagnetic radiation at a frequency characteristic of the isotope. The sensitivity and signal strength of CNMR spectra were all increased in the skeleton ^{13}C-enriched fullerenes, while their chemical shifts were not changed in ^{13}C-enriched C_{60}/C_{70} (Fig 3). The peak corresponding to ^{13}C-enriched C_{70}/C_{60} and C_{70}/C_{60} are all the same positions, which were in excellent agreement with the results reported by other group.[55, 57, 58]

From the results of CNMR spectra, we did not observe that the symmetry of molecular structure was altered or destroyed due to ~7% ^{13}C incorporating into the skeleton carbon cage of fullerenes, only showing signal enhancement of spectra and reducing the data acquisition time to a feasible 3 days despite low solubility.[75, 76] The signal strength of CNMR in ^{13}C-enriched C_{70}/C_{60} indicated about 8-fold increases with five ^{13}C-substituted in a fullerene carbon cage. As expected, the proton NMR spectra of the samples dissolved in toluene-d_8 were devoid of any absorption besides the $C_6D_5CD_3$ peak at 137.11 ppm. In brief, it was the typical characteristics that the introduction of ^{13}C enlarged the signal of CNMR of fullerenes, and enhanced the detection sensitivity of CNMR. The signal enhancement of fullerenes nanomaterials CNMR would provide the potential for the development of new analytical methods.

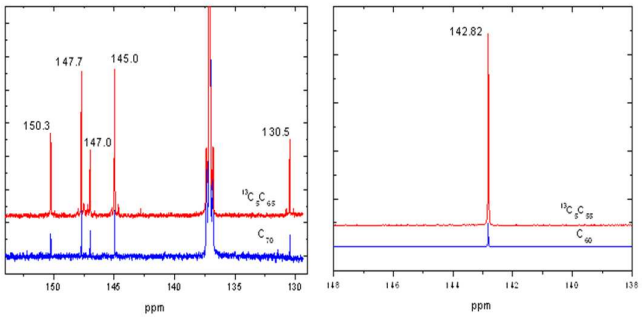

Fig. 3. NMR spectra of ^{13}C-enriched fullerenes and unlabeled fullerenes.

IR and Raman analysis

IR and Raman spectra are both molecular vibration spectra which reveal the characters of molecular structure. Compared to ^{12}C, ^{13}C has a relative heavy atomic weight of 13, which is made up of 6 protons and 7 neutrons. The introduction of the heavy atom ^{13}C would likely change the molecular vibrations of fullerene. The IR results revealed that the ^{13}C-enriched C_{70} retained all the characteristic bands of $^{12}C_{70}$ and showed a trend that with the increase of intruded ^{13}C atoms the absorption bands shifted to lower wavenumbers slightly (Table 2). Compared to C_{60}, the molecular symmetry of C_{70} and ^{13}C-enriched C_{70} was lower. Their IR spectra were relative complicated. The introduced ^{13}C atoms did not cause the strong changes of the IR spectra and made the most characteristic peak shift from 1427 cm^{-1} to 1423 cm^{-1} (Fig. 4).

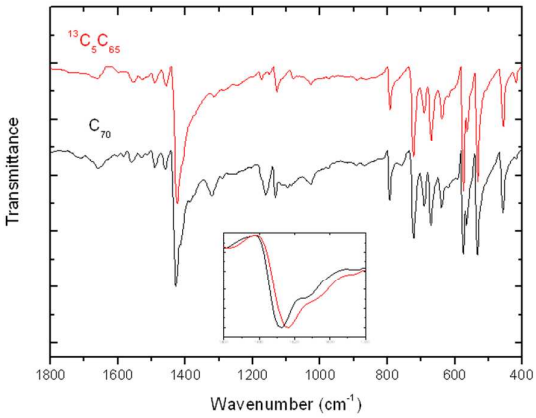

Fig. 4. IR spectra of $^{13}C_5C_{65}$ and C_{70}.

Table 2. Displacement of IR characteristic peaks of C_{70} and $^{13}C_5C_{65}$.

	C_{70}	$^{13}C_5C_{65}$
ν_{IR}/cm^{-1}	1427.3	1423.4
	1132.2	1128.3
	792.7	792.7
	723.3	723.3
	671.2	669.3
	574.8	574.8
	532.3	532.3
	457.1	455.2

For ^{13}C-enriched C_{60}, the little addition of ^{13}C atoms also did not change the four vibration modes, but made the characteristic bands shift down observably.[69]

The Raman spectra of ^{13}C-enriched C_{70} exerted regular changes and were shown in Fig. 5. For C_{70}, the Raman spectra showed 12 obvious characteristic peaks at 258.6, 701.4, 737.7, 770.6, 1061.1, 1184.0, 1229.2, 1332.8, 1368.0, 1447.2, 1513.6 and 1566.1 cm^{-1}.[77] The strongest peak was at about 1566.1 cm^{-1}. For $^{13}C_5C_{65}$, five intruded ^{13}C atoms did not alter the Raman vibrational modes of C_{70}, without new characteristic peak, only made characteristic peaks shift down 3-4 wavenumbers (Table 3). In view of the lower molecular symmetry of C_{70}, a few introduced ^{13}C atoms may be not enough to cause the strong alterations in the molecular vibration spectra of high carbon cage-based fullerenes. More invaded atoms exacerbated the change of symmetry reducing the degeneracy and triggered some new characteristic peaks potentially. But for the lower molecular symmetry of high carbon cage-based fullerenes, the ^{13}C stable isotope effects were possibly relative weak and not easily altered or damaged the intrinsic structure of fullerenes. IR and Raman spectra showed that the invaders ^{13}C did not change the overall structure of fullerenes. But in our previous investigations, with increased amount of ^{13}C, the Raman spectra of ^{13}C-enriched C_{60} shifted into lower wavenumber, Raman silent mode was activated and new vibrational peaks emerged.[69] These changes were due to the mass addition caused by the incorporation of ^{13}C atoms which broke easily the high symmetry structure of C_{60}.

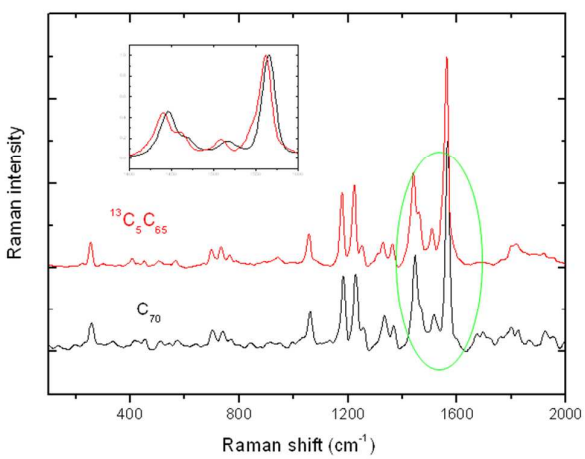

Fig. 5. Raman spectra of $^{13}C_5C_{65}$ and C_{70}.

Table 3. Displacement of Raman characteristic peaks of C_{70} and $^{13}C_5C_{65}$.

	ν_{Raman}/cm^{-1}				
C_{70}	258.6				
	701.4	737.7	770.6		
	1061.1	1184.0	1229.2	1332.8	1368.0
	1447.2	1513.6	1566.1		
$^{13}C_5C_{65}$	255.4				
	698.3	733.0	765.9		
	1055.0	1180.0	1223.3	1328.4	1362.2
	1441.4	1507.8	1563.3		

Electrochemical analysis

Electrochemical measurements are the main methods to characterize the electronic properties of fullerenes and their derivatives. Fig. 6 showed the electrochemical properties of purified C_{70} and the ^{13}C-enriched C_{70} samples. Three reversible electron reduction waves were observed, which verified the good electron withdrawing ability of C_{70} molecules. These results were similar with the reported of the references.[78-81] The cyclic voltammogram of ^{13}C-enriched C_{70} showed clearly positive shift relative to unlabelled C_{70}. Incorporation of the stable isotopes ^{13}C in fullerene molecular significantly influenced the half-wave potentials of C_{70}. The electron affinity of ^{13}C-enriched C_{70} should be weaker than that of unlabeled C_{70} in redox process. These diversities may be due to the addition of ^{13}C and caused the HOMO-LUMO energy difference between C_{70} and ^{13}C-enriched C_{70}, altered the C_{70} molecular strain and reduced the degree of conjugation of molecules. This isotope effect of electrochemical properties in fullerene C_{70} has not been reported yet. These data again demonstrated that the labeled ^{13}C atoms break the mass distribution and change the electron configuration of C_{70} molecule.

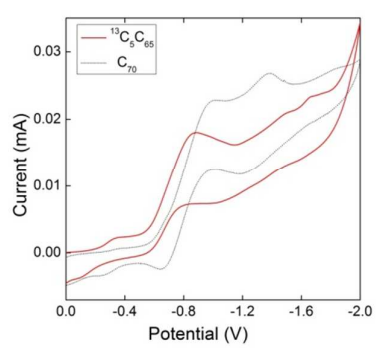

Fig. 6. Cyclic voltammogram of $^{13}C_5C_{65}$ and C_{70}.

Conclusions

In the present work, ^{13}C-enriched large carbon cage-based fullerenes were synthesized in a large scale by arc discharge method. The direct stable isotope ^{13}C labeling on the skeleton of fullerenes retained their intrinsic structures. Stable isotopes were randomly distributed in the carbon cage. The ^{13}C labeled amounts of C_{70} was higher than that of natural abundance, which greatly improved the ^{13}C detection signal strength in IRMS, and also enhanced the signal strength and sensitivity of fullerenes for CNMR. MS spectra showed that isotopic effects were fitted with Poisson distribution. In the arc-discharge experiment, the ^{13}C stable isotopic effects were seemed to be weaker with increasing size of fullerenes carbon cages, especially for their molecular vibration spectra. Simultaneously, some ^{13}C-enriched high carbon fullerenes (such as ^{13}C-C_{76}, C_{82} and C_{96} etc.) were also existed in the arc-discharge. The mechanism of fullerenes formation in the process of arc-discharge was speculated by contrast ^{13}C labeled amounts and isotopic effects between ^{13}C-enriched C_{70} and those of ^{13}C-enriched C_{60}. The skeleton ^{13}C-labeling technique would understand fully the formation mechanism of fullerenes and other carbon materials. Relying on the diversity spectroscopic methods and IRMS, ^{13}C stable isotope labeling methods provide us a convenient and safer way to reflect the real properties of C_{70} in biological systems. Although, due to the expensive pure ^{13}C power the manufacture cost of ^{13}C-enriched C_{70} is very high. It is also worth to note that the amount for a tracing experiment in vivo is small, usually less than 50 mg, and the detection sensitivity of IRMS for ^{13}C is very high.[48-50] Thererfore, the introduction of stable isotope labeling technique makes the biomedical effect researches of fullerene nanomaterials more safe and effective comparing with radioactive marker.[82-86] We have confidence that the stable isotope labeling provides the new analytical method of the in vivo quantitative and intrinsic detection for carbon nanomaterials and can be widely used in the nanomedical fields of fullerene-based nanomaterials and other carbon materials.

Acknowledgements

This work was supported by the National Natural Science Foundation of China (Nos. 11475194, 11005116 and 21307101), Beijing Natural Science Foundation（2152038） and the National Basic Research Program of China (973 program: 2012CB932601 and 2013CB932703). We thank Mrs. Ping Liang at Analytical and testing center, Huazhong University of Science & Technology, for the CNMR analyses.

Notes and references

1 A. Kleiman-Shwarsctein, T. F. Jaramillo, S.-H. Baeck, M. Sushchikh and E. W. McFarland, *J Electrochem Soc*, 2006, **153**, C483-C487.
2 C. Lorenz, N. Von Goetz, M. Scheringer, M. Wormuth and K. Hungerbühler, *Nanotoxicology*, 2011, **5**, 12-29.
3 P. Avouris, Z. Chen and V. Perebeinos, *Nat Nanotechnol*, 2007, **2**, 605-615.
4 M. Ferrari, *Nat Rev Cancer*, 2005, **5**, 161-171.
5 J. Lee, Y. Mackeyev, M. Cho, D. Li, J.-H. Kim, L. J. Wilson and P. J. Alvarez, *Environ Sci Technol*, 2009, **43**, 6604-6610.
6 R. Partha and J. L. Conyers, *Int J Nanomed*, 2009, **4**, 261-275.
7 P. Chaudhuri, A. Paraskar, S. Soni, R. A. Mashelkar and S. Sengupta, *Acs Nano*, 2009, **3**, 2505-2514.
8 S. Osuna, M. Swart and M. Solà, *Chem-Eur J*, 2010, **16**, 3207-3214.
9 Y. Doi, A. Ikeda, M. Akiyama, M. Nagano, T. Shigematsu, T. Ogawa, T. Takeya and T. Nagasaki, *Chem-Eur J*, 2008, **14**, 8892-8897.
10 A. Ikeda, M. Matsumoto, M. Akiyama, J.-i. Kikuchi, T. Ogawa and T. Takeya, *Chem Commun*, 2009, 1547-1549.
11 Q. Liu, M. Guan, L. Xu, C. Shu, C. Jin, J. Zheng, X. Fang, Y. Yang and C. Wang, *Small*, 2012, **8**, 2070-2077.
12 Q. Liu, X. Zhang, X. Zhang, G. Zhang, J. Zheng, M. Guan, X. Fang, C. Wang and C. Shu, , 2013, **5**, 11101-11107.
13 M. Mikawa, H. Kato, M. Okumura, M. Narazaki, Y. Kanazawa, N. Miwa and H. Shinohara, *Bioconjugate Chem*, 2001, **12**, 510-514.
14 J. Zhang, K. M. Liu, G. M. Xing, T. X. Ren and S. K. Wang, *J Radioanal Nucl Chem*, 2007, **272**, 605-609.
15 G. M. Xing, H. Yuan, R. He, X. Y. Gao, L. Jing, F. Zhao, Z. F. Chai and Y. L. Zhao, *J Phys Chem B*, 2008, **112**, 6288-6291.
16 C. Y. Chen, G. M. Xing, J. X. Wang, Y. L. Zhao, B. Li, J. Tang, G. Jia, T. C. Wang, J. Sun, L. Xing, H. Yuan, Y. X. Gao, H. Meng, Z. Chen, F. Zhao, Z. F. Chai and X. H. Fang, *Nano Lett*, 2005, **5**, 2050-2057.
17 X.-J. Liang, H. Meng, Y. Z. Wang, H. Y. He, J. Meng, J. Lu, P. C. Wang, Y. L. Zhao, X. Y. Gao, B. Y. Sun, C. Y. Chen, G. M. Xing, D. W. Shen, M. M. Gottesman, Y. Wu, J.-J. Yin and L. Jia, *P Natl Acad Sci USA*, 2010, **107**, 7449-7454.
18 H. Meng, G. M. Xing, B. Y. Sun, F. Zhao, H. Lei, W. Li, Y. Song, Z. Chen, H. Yuan, X. X. Wang, J. Long, C. Y. Chen, X. J. Liang, N. Zhang, Z. F. Chai and Y. L. Zhao, *ACS Nano*, 2010, **4**, 2773-2783.
19 X.-L. Chang, S.-T. Yang and G. M. Xing, *J Biomed Nanotechnol*, 2014, **10**, 2828-2851.
20 A. Nel, T. Xia, L. Mädler and N. Li, *Science*, 2006, **311**, 622-627.
21 G. Oberdörster, E. Oberdörster and J. Oberdörster, *Environ Health Persp*, 2005, **113**, 823-839.
22 G. Oberdörster, *J Intern Med*, 2010, **267**, 89-105.
23 M. Uo, T. Akasaka, F. Watari, Y. Sato and K. Tohji, *Dent Mater J*, 2011, **30**, 245-263.
24 H. Wang, S.-T. Yang, A. Cao and Y. Liu, *Accounts Chem Res*, 2012, **46**, 750-760.
25 R. Bullard-Dillard, K. E. Creek, W. A. Scrivens and J. M. Tour, *Bioorg Chem*, 1996, **24**, 376-385.
26 J.-Y. Xu, Q.-N. Li, J.-G. Li, T.-C. Ran, S.-W. Wu, W.-M. Song, S.-L. Chen and W.-X. Li, *Carbon*, 2007, **45**, 1865-1870.
27 S. Yamago, H. Tokuyama, E. Nakamura, K. Kikuchi, S. Kananishi, K. Sueki, H. Nakahara, S. Enomoto and F. Ambe, *Chem Biol*, 1995, **2**, 385-389.
28 S. C. J. Sumner, T. R. Fennell, R. W. Snyder, G. F. Taylor and A. H. Lewin, *J Appl Toxicol*, 2010, **30**, 354-360.
29 H. Song, S. Luo, H. Wei, H. Song, Y. Yang and W. Zhao, *J Radioanal Nucl Chem*, 2010, **285**, 635-639.
30 Y. G. Li, X. Huang, R. L. Liu, Q. N. Li, X. D. Zhang and W. X. Li, *J Radioanal Nucl Chem*, 2005, **265**, 127-131.
31 N. Nadežda, V.-Đ. Sanja, J. Drina, Đ. Divna, M. Marija, B. Nataša and T. Vladimir, *Nanotechnology*, 2009, **20**, 385102.
32 Q. N. Li, Y. Xiu, X. D. Zhang, R. L. Liu, Q. Q. Du, X. G. Shun, S. L. Chen and W. X. Li, *Nucl Med Biol*, 2002, **29**, 707-710.

33 J. Tang, G. M. Xing, H. Yuan, W. B. Cao, L. Jing, X. F. Gao, L. Qu, Y. Cheng, C. Ye, Y. L. Zhao, Z. F. Chai, K. Ibrahim, H. J. Qian and R. Su, *J Phys Chem B*, 2005, **109**, 8779-8785.
34 J. Tang, G. M. Xing, Y. L. Zhao, L. Jing, X. F. Gao, Y. Cheng, H. Yuan, F. Zhao, Z. Chen, H. Meng, H. Zhang, H. J. Qian, R. Su and K. Ibrahim, *Adv Mater*, 2006, **18**, 1458-1462.
35 J. Tang, G. M. Xing, H. Yuan, X. F. Gao, L. Jing, S. K. Wang, Y. Cheng and Y. L. Zhao, *J Radioanal Nucl Chem*, 2007, **272**, 307-310.
36 J. Tang, G. M. Xing, F. Zhao, H. Yuan and Y. L. Zhao, *J Nanosci Nanotechno*, 2007, **7**, 1085-1101.
37 J. Tang, G. M. Xing, Y. L. Zhao, L. Jing, H. Yuan, F. Zhao, X. Y. Gao, H. J. Qian, R. Su, K. Ibrahim, W. G. Chu, L. N. Zhang and K. Tanigaki, *J Phys Chem B*, 2007, **111**, 11929-11934.
38 S. X. Zhao, J. Zhang, J. Q. Dong, B. K. Yuan, X. H. Qiu, S. Yang, J. Hao, H. Zhang, H. Yuan, G. M. Xing, Y. L. Zhao and B. Y. Sun, *J Phys Chem C*, 2011, **115**, 6265-6268.
39 S. X. Zhao, J. Zhang, X. H. Guo, X. H. Qiu, J. Q. Dong, B. K. Yuan, K. Ibrahim, J. O. Wang, H. J. Qian, Y. L. Zhao, S. Y. Yang, J. Hao, H. Zhang, H. Yuan, G. M. Xing and B. Y. Sun, *Nanoscale*, 2011, **3**, 4130-4134.
40 J. Zhang, S. X. Zhao, B. K. Yuan, K. Deng, B. Y. Sun and X. H. Qiu, *Surf Sci*, 2012, **606**, 78-82.
41 J. Eagles, S. J. Fairweather-Tait and R. Self, *Anal Chem*, 1985, **57**, 469-471.
42 B. Gulson and H. Wong, *Environ Health Persp*, 2006, **114**, 1486-1488.
43 M. Li, W. E. Huang, C. M. Gibson, P. W. Fowler and A. Jousset, *Anal Chem*, 2012, **85**, 1642-1649.
44 A. Mutlib, R. Espina, J. Atherton, J. Wang, R. Talaat, J. Scatina and A. Chandrasekaran, *Chem Res Toxicol*, 2012, **25**, 572-583.
45 A. E. Mutlib, *Chem Res Toxicol*, 2008, **21**, 1672-1689.
46 M.-N. Croteau, D. J. Cain and C. C. Fuller, *Environ Sci Technol*, 2013, **47**, 3424-3431.
47 B. Gulson, M. McCall, M. Korsch, L. Gomez, P. Casey, Y. Oytam, A. Taylor, M. McCulloch, J. Trotter and L. Kinsley, *Toxicol Sci*, 2010, **118**, 140-149.
48 S. T. Yang, W. Guo, Y. Lin, X. Y. Deng, H. F. Wang, H. F. Sun, Y. F. Liu, X. Wang, W. Wang, M. Chen, Y. P. Huang and Y. P. Sun, *J Phys Chem C*, 2007, **111**, 17761-17764.
49 S. T. Yang, K. A. S. Fernando, J. H. Liu, J. Wang, H. F. Sun, Y. F. Liu, M. Chen, Y. P. Huang, X. Wang, H. F. Wang and Y. P. Sun, *Small*, 2008, **4**, 940-944.
50 X.-L. Chang, L. Ruan, S.-T. Yang, B. Sun, C. Guo, L. Zhou, J. Dong, H. Yuan, G. Xing, Y. Zhao and M. Yang, *Environ Sci: Nano*, 2014, **1**, 64-70.
51 Z. Muccio and G. P. Jackson, *Analyst*, 2009, **134**, 213-222.
52 L. A. Gregoricka, *Am J Phys Anthropol*, 2013, **152**, 353-369.
53 S. Benson, C. Lennard, P. Maynard and C. Roux, *Forensic Sci Int*, 2006, **157**, 1-22.
54 W. Krätschmer, K. Fostiropoulos and D. R. Huffman, *Chem Phys Lett*, 1990, **170**, 167-170.
55 G. Meijer and D. S. Bethune, *J Chem Phys*, 1990, **93**, 7800-7802.
56 J. M. Hawkins, A. Meyer, S. Loren and R. Nunlist, *J Am Chem Soc*, 1991, **113**, 9394-9395.
57 C. S. Yannoni, P. P. Bernier, D. S. Bethune, G. Meijer and J. R. Salem, *J Am Chem Soc*, 1991, **113**, 3190-3192.
58 C. C. Chen and C. M. Lieber, *J Am Chem Soc*, 1992, **114**, 3141-3142.
59 T. W. Ebbesen, J. Tabuchi and K. Tanigaki, *Chem Phys Lett*, 1992, **191**, 336-338.
60 J. M. Hawkins, *Accounts Chem Res*, 1992, **25**, 150-156.
61 R. D. Johnson, D. S. Bethune and C. S. Yannoni, *Accounts Chem Res*, 1992, **25**, 169-175.
62 M. C. Martin, J. Fabian, J. Godard, P. Bernier, J. M. Lambert and L. Mihaly, *Phys Rev B*, 1995, **51**, 2844-2847.
63 P. J. Horoyski, M. L. W. Thewalt and T. R. Anthony, *Phys Rev B*, 1996, **54**, 920-929.
64 P. W. Dunk, N. K. Kaiser, C. L. Hendrickson, J. P. Quinn, C. P. Ewels, Y. Nakanishi, Y. Sasaki, H. Shinohara, A. G. Marshall and H. W. Kroto, *Nat Commun*, 2012, **3**, 855(1-9).
65 Z. Wang, X. L. Chang, Z. H. Lu, M. Gu, Y. L. Zhao and X. F. Gao, *Chem Sci*, 2014, **5**, 2940-2948.
66 W. Kratschmer, L. D. Lamb, K. Fostiropoulos and D. R. Huffman, *Nature*, 1990, **347**, 354-358.
67 R. E. Haufler, J. Conceicao, L. P. F. Chibante, Y. Chai, N. E. Byrne, S. Flanagan, M. M. Haley, S. C. O'Brien, C. Pan, Z. Xiao, W. E. Billups, M. A. Ciufolini, R. H. Hauge, J. L. Margrave, L. J. Wilson, R. F. Curl and R. E. Smalley, *J Phys Chem*, 1990, **94**, 8634-8636.
68 Z. N. Gu, J. X. Qian, X. H. Zhou, Y. Q. Wu, X. Zhu, S. Q. Feng and Z. Z. Gan, *J Phys Chem*, 1991, **95**, 9615-9618.
69 L. F. Ruan, X. L. Chang, B. Y. Sun, C. B. Guo, J. Q. Dong, S. T. Yang, X. F. Gao, Y. L. Zhao and M. Yang, *Chin Sci Bull*, 2014, **59**, 905-912.
70 R. D. Johnson, G. Meijer, J. R. Salem and D. S. Bethune, *J Am Chem Soc*, 1991, **113**, 3619-3621.
71 J. M. Hawkins, S. Loren, A. Meyer and R. Nunlist, *J Am Chem Soc*, 1991, **113**, 7770-7771.
72 R. Tycko, R. C. Haddon, G. Dabbagh, S. H. Glarum, D. C. Douglass and A. M. Mujsce, *J Phys Chem*, 1991, **95**, 518-520.
73 C. S. Yannoni, R. D. Johnson, G. Meijer, D. S. Bethune and J. R. Salem, *J Phys Chem*, 1991, **95**, 9-10.
74 R. D. Johnson, G. Meijer and D. S. Bethune, *J Am Chem Soc*, 1992, **112**, 8983-8984.
75 H. Ajie, M. M. Alvarez, S. J. Anz, R. D. Beck, F. Diederich, K. Fostiropoulos, D. R. Huffman, W. Kraetschmer, Y. Rubin, K. E. Schriver, D. Sensharma and R. L. Whetten, *J Phys Chem*, 1990, **94**, 8630-8633.
76 R. Taylor, J. P. Hare, A. K. Abdulsada and H. W. Kroto, *J Chem Soc, Chem Commun*, 1990, 1423-1424.
77 D. S. Bethune, G. Meijer, W. C. Tang, H. J. Rosen, W. G. Golden, H. Seki, C. A. Brown and M. S. de Vries, *Chem Phys Lett*, 1991, **179**, 181-186.
78 P.M. Allemand, A. Koch, F. Wudl, Y. Rubin, F. Diederich, M.M. Alvarez, S.J. Anz and R.L. Whetten, *J Am Chem Soc*, 1991, **113,** 1050-1051.
79 D.M. Cox, S. Behal, M. Disko, S.M. Gorun, M. Greaney, C.S. Hsu, E.B. Kollin, J. Millar and J. Robbins, *J Am Chem Soc*, 1991, **113**, 2940-2944.
80 D. Dubois, G. Moninot, W. Kutner, M.T. Jones, and K.M. Kadish, *J Phys Chem*, 1992, **96**, 7137-7145.
81 Q. Xie, E. Perez-Cordero, and L. Echegoyen, *J Am Chem Soc*, 1992,**114**, 3978-3980.
82 J. H. Liu, S. T. Yang, X. Wang, H. Wang, Y. Liu, P. G. Luo, Y. Liu and Y. P. Sun, *ACS Appl Mater Interfaces*, 2014, **6**, 14672-14678.
83 S. K. Hanna, R. J. Miller and H. S. Lenihan, *J Hazard Mater*, 2014, **279**, 32-37.
84 K. M. Schreiner, T. R. Filley, R. A. Blanchette, B. B. Bowen, R. D. Bolskar, W. C. Hockaday, C. A. Masiello and J. W. Raebiger, *Environ Sci Technol*, 2009, **43**, 3162-3168.
85 Z. Liu, X. Li, S. M. Tabakman, K. Jiang, S. Fan and H. Dai, *J Am Chem Soc*, 2008, **130**, 13540-13541.
86 C. W. Isaacson, C. Y. Usenko, R. L. Tanguay and J. A. Field, *Anal Chem*, 2007, **79**, 9091-9097.

RSC Advances

ARTICLE

Fig. 1. Separation and purification of ^{13}C-enriched fullerenes.

Fig. 2. MS spectra of C_{70} and ^{13}C-C_{70}.

Fig. 3. NMR spectra of ^{13}C-enriched fullerenes and unlabeled fullerenes.

Fig. 4. IR spectra of $^{13}C_5C_{65}$ and C_{70}.

Fig. 5. Raman spectra of $^{13}C_5C_{65}$ and C_{70}.

Fig. 6. Cyclic voltammogram of $^{13}C_5C_{65}$ and C_{70}.

Table 1. ^{13}C/^{12}C isotope ratios of ^{13}C-enriched C_{70}.

Table 2. Displacement of IR characteristic peaks of C_{70} and $^{13}C_5C_{65}$.

Table 3. Displacement of Raman characteristic peaks of C_{70} and $^{13}C_5C_{65}$.

RSC Advances

ARTICLE

Chang et al. Fig. 1.

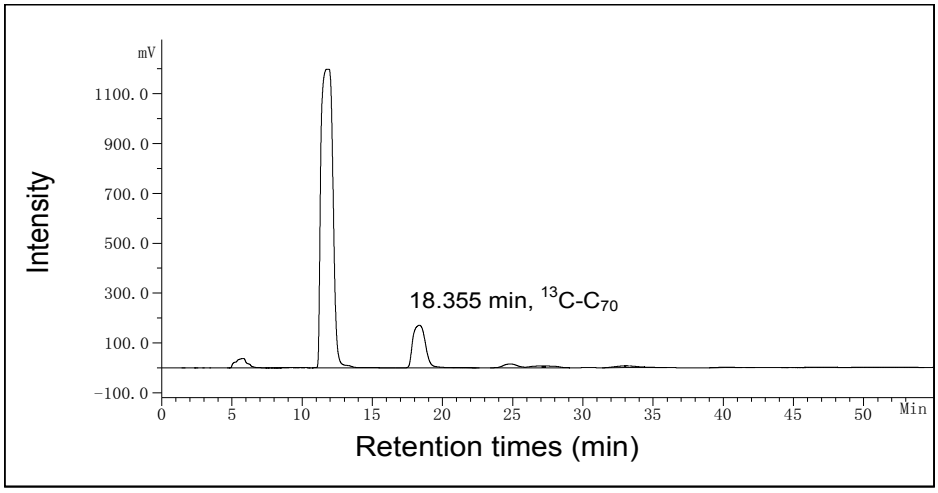

Chang et al. Fig. 2.

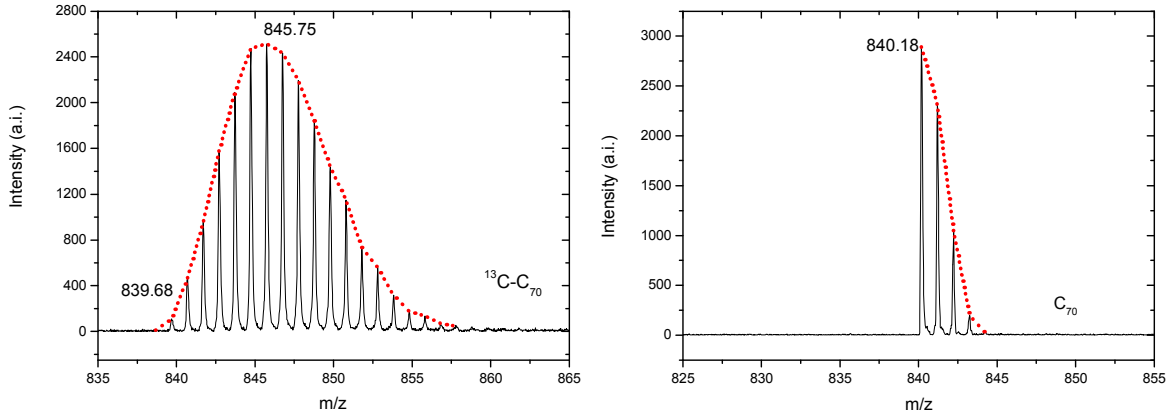

Chang et al. Fig. 3.

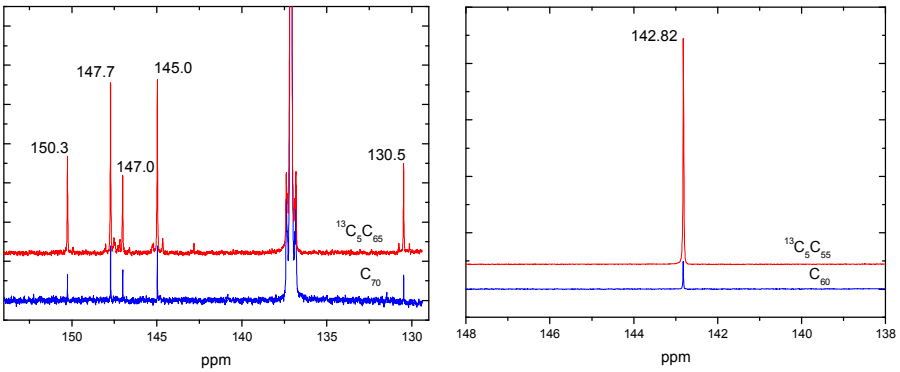

Chang et al. Fig. 4.

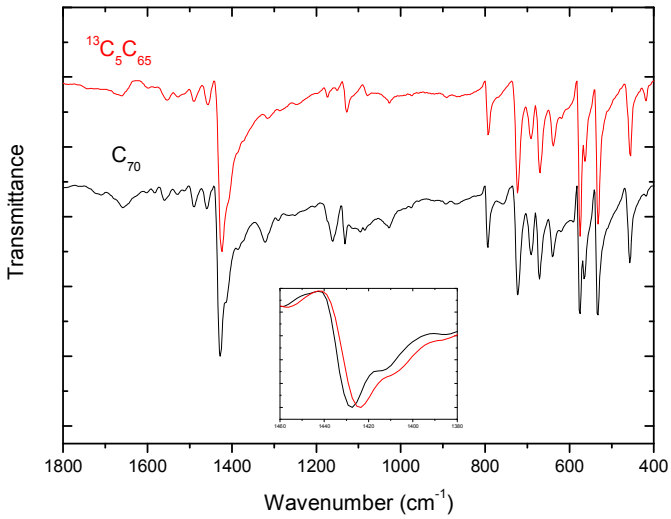

Chang et al. Fig. 5.

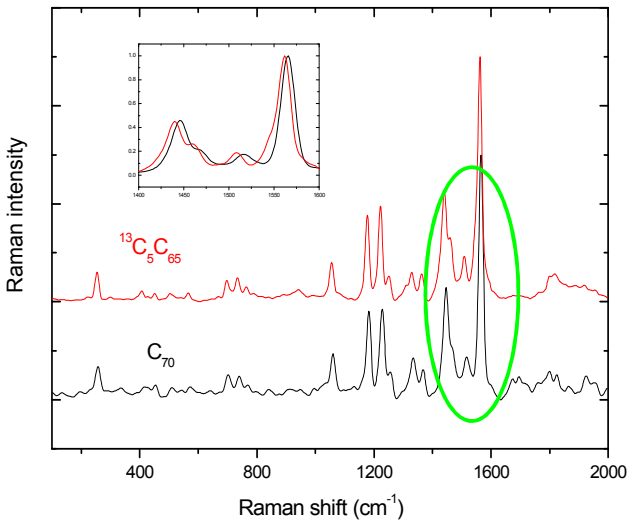

Chang et al. Fig. 6.

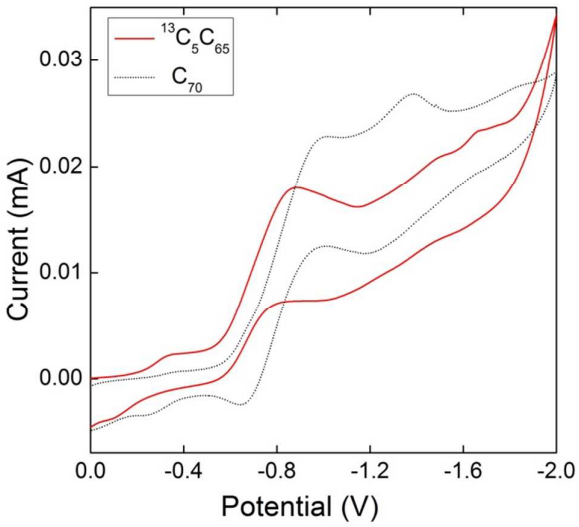

Chang et al. Table 1.

The addition of ^{13}C in raw carbon powder (%)	$\delta^{13}C/^{12}C$	$^{13}C/^{12}C$ (%)	^{13}C-enriched C_{70}
0	-17.436	1.087	C_{70}
5	2883.265	4.161	$^{13}C_3C_{67}$
15	7211.047	8.408	$^{13}C_5C_{65}$

Chang et al. Table 2.

	C_{70}	$^{13}C_5C_{65}$
ν_{IR}/cm^{-1}	1427.3	1423.4
	1132.2	1128.3
	792.7	792.7
	723.3	723.3
	671.2	669.3
	574.8	574.8
	532.3	532.3
	457.1	455.2

Chang et al. Table 3.

87

	ν_{Raman}/cm^{-1}				
C_{70}	258.6				
	701.4	737.7	770.6		
	1061.1	1184.0	1229.2	1332.8	1368.0
	1447.2	1513.6	1566.1		
$^{13}C_5C_{65}$	255.4				
	698.3	733.0	765.9		
	1055.0	1180.0	1223.3	1328.4	1362.2
	1441.4	1507.8	1563.3		